Available online at www.sciencedirect.com
SCIENCE DIRECT®
Chemical Physics Letters 397 (2004) 138–143
CHEMICAL PHYSICS LETTERS
www.elsevier.com/locate/cplett

Structure of solid-supported lipid–DNA–metal complexes investigated by energy dispersive X-ray diffraction

G. Caracciolo [a], C. Sadun [a], R. Caminiti [a,*], M. Pisani [b], P. Bruni [b], O. Francescangeli [c]

[a] *Dipartimento di Chimica and INFM, Università 'La Sapienza', P.le A. Moro 5, 00185 Rome, Italy*
[b] *Dipartimento di Scienze dei Materiali e del Territorio and INFM, Università Politecnica delle Marche, Via Brecce Bianche, 60131 Ancona, Italy*
[c] *Dipartimento di Fisica e Ingegneria dei Materiali e del Territorio and INFM, Università Poitecnica delle Marche, Via Brecce Bianche, 60131 Ancona, Italy*

Received 30 July 2004; in final form 30 July 2004
Available online 11 September 2004

Abstract

When mixing aqueous solutions of DNA and dioloeyl-phosphatidylcholine multilamellar liposomes in the presence of Mn^{2+} ions, a multilamellar liquid-crystalline phase is formed in which DNA monolayers are comprised between opposing lipid bilayers. Here, we report on a new experimental procedure resulting in the formation of solid-supported DOPC–DNA–Mn^{2+} complexes in the biologically relevant excess water condition. The supramolecular structure of solid-supported complexes, characterized by means of Energy Dispersive X-ray Diffraction, exhibits very similar structural properties with respect to the solution structure of the complexes as revealed by synchrotron Small Angle X-ray Scattering measurements.

1. Introduction

Cationic liposomes (CLs), binary mixtures of cationic and zwitterionic lipids, are extensively used as DNA-carriers in human gene therapy in which context they are usually named lipoplexes [1–3]. When CLs and DNA are mixed, self-assembled aggregates spontaneously form in which cationic lipids act as DNA condensing agents. The driving force for DNA complexation is the entropic gain arising from the release of the charged counterions condensed both onto the lipid and the DNA [4,5]. By using small angle X-ray scattering (SAXS) and synchrotron X-ray diffraction (XRD), the microscopic inner structure of lipoplexes has been recently elucidated [6–11].

The cationic lipid/DNA charge ratio and the net positive charge of the complexes are both key parameters which can promote their association with the negatively charged cell surface [12]. A straight relationship between the chemical nature of the cationic lipids and their ability to transfect and to develop cytotoxicity has also been evidenced but not entirely clarified. The cationic lipid headgroup often consists of primary, secondary or tertiary amines joined via a linker to a large hydrophobic domain. The role played by the neutral helper lipid is also important because it controls the morphologies and structures of the composite condensates and affects the DNA transfection efficiency sometimes dramatically [13,14]. Depending on the structural and morphological properties of the zwitterionic helper lipid, either a liquid-crystalline lamellar or a two-dimensional (2D) inverted hexagonal phase can be obtained [15].

Despite of the several recognized advantages in the use of lipoplexes in vivo and in vitro transfection, the low transfection efficiency, cytotoxicity and immunogenic response associated with the use of cationic surfactants are the major drawbacks that limit their use as potential gene delivery vectors.

* Corresponding author. Fax: + 39 06 490631.
E-mail address: r.caminiti@caspur.it (R. Caminiti).

0009-2614/$ - see front matter © 2004 Elsevier B.V. All rights reserved.
doi:10.1016/j.cplett.2004.08.102

To overcome these difficulties, new formulations have been tested based on the exclusive use of neutral lipids which are not-cytotoxic. In these complexes, divalent electrolyte counterions common in biological cells (Mn^{2+}, Ca^{2+}, Co^{2+}, Mg^{2+}, Fe^{2+}) are used as DNA condensing agents [16–20]. Neutral liposomes (L) and divalent metal cations (Me^{2+}) successfully behave as cationic liposomes condensing DNA and promoting the formation of stable ternary L–DNA–Me^{2+} complexes. These biomaterials are expected to exhibit lower inherent cytotoxicity than CLs. On the other hand, addition of metal cations leads to the formation of complexes that are more stable than binary L–DNA complexes.

Some of us recently investigated the structural and morphological properties of triple complexes formed by dioloeyl phosphatidylcholine (DOPC), DNA and Mn^{2+} revealing the existence of a multilayered structure made of alternating lipid bilayers and DNA monolayers similar to the lamellar liquid-crystalline L_{α}^{c} phase found in lipoplexes [20].

In this Letter we report, for the first time, on the structural properties of solid-supported (DOPC)–DNA–Mn^{2+} triple complex fully hydrated from a vapor-saturated atmosphere as revealed by Energy Dispersive X-ray Diffraction (EDXD). Even if lipid/DNA complexes dispersed in aqueous solutions are a frequent measurement condition, solid-supported samples are emerging as a significative alternative to achieve structural information. Specifically, in view of the recent overcoming of the vapor pressure paradox by Katsaras [21,22], solid-supported lipid multibilayers systems fully hydrated from vapor have been found to exhibit the same physico-chemical properties of unoriented liposomes in aqueous solution and therefore represent excellent model systems of biological membranes. Higher experimental resolution and shorter acquisition times are the main advantages in using solid-supported systems with respect to their counterpart in solution. Comparing our EDXD structural findings with those obtained on the DOPC–DNA–Mn^{2+} complex in aqueous solution by synchrotron SAXS, here we prove that the inner structure of solid-supported DOPC–DNA–Mn^{2} complexes fully hydrated from vapor is essentially the same with respect to the solution structure of the complexes immersed in water.

2. Materials and methods

2.1. Sample preparation

The liposomes were prepared dissolving the appropriate amounts of DOPC in chloroform and removing the solvent under a stream of nitrogen; the dried film was put in a vacuum for 2 h to remove remnant traces of the solvent. The 4-(2-hydroxyl)piperazine-1-ethanesulphonic acid (HEPES) buffer (20 mM, pH 7.2) was added to give a lipid concentration of 0.14% (w/w). The multilamellar vesicles (MLVs) were prepared vortexing the lipid suspension several times during the hydration period (4 h), and leaving then this suspension to equilibrate for 1 day.

The triple complexes were prepared by mixing equal volumes of the MLV lipid suspension (1.78 mM), DNA (2.4 mM), from calf thymus, and metal ion Mn^{2+} as chloride (7 mM). The triple DOPC:DNA:Mn^{2+} complex is prepared at molar ratio 3:4:12. The concentration of DNA is reported as phosphate units. DOPC was purchased from Avanti Polar Lipids, the DNA and the metal ions were purchased from Fluka.

2.2. EDXD and SAXS experiments

2.2.1. EDXD measurements

Reflection-mode EDXD experiments were carried out using a non conventional apparatus elsewhere described [23,24]. Briefly, an incident polychromatic X-ray radiation is used and the diffracted beam is energy resolved by a solid state detector located at a suitable scattering angle. The diffractometer operates in vertical θ/θ geometry and is equipped with an X-ray generator (W target), a collimating system, step motors, and a solid-state detector connected via an electronic chain to a multichannel analyzer. Both the X-ray tube and the detector can rotate around their common center where a cell is placed. After a preliminary set of measurements, one scattering angle $\theta = 0.45°$ was selected to investigate the interesting range of the reciprocal space. The diffracted intensity is measured as a function of the transfer momentum q ($q = \cos t^{*}E^{*}\sin\theta$; $\cos t = 1.01354$ Å^{-1} keV^{-1}). A Drop of 100 μl of the lipid solution was carefully spread onto the freshly-cleaved surface of $\langle 1\,0\,0\rangle$ oriented silicon wafers. The spread drop was allowed to dry over about 1 h up to a uniform dry film was obtained. After positioning the sample in the X-ray chamber, the dry lipid film was fully hydrated by vapor. The lipid hydration kinetics was followed in time due to the peculiar characteristics of EDXD. Each EDXD scan was collected at room temperature for $t = 2$ s. In the case of the triple complex, the same experimental procedure was applied. The dry film was carefully hydrated by vapor up to traces of water condensation onto the support were evident. At this point, the system was in the biologically relevant excess water condition. Then, it was let to equilibrate for $t = 72$ h. EDXD scan of the solid-supported triple complex was collected for $t = 1000$ s. During such period no damage to biological samples occur as elsewhere discussed [25].

2.2.2. Synchrotron SAXS measurements

SAXS was carried out at beamline ID02 at the European Synchrotron Radiation Facility (Grenoble,

France). The detector distance was 1.2 m and the wavelength of X-ray was $\lambda = 0.995$ Å. The diffraction patterns were collected using a 2D CCD detector. The sample was held in a 1mm size quartz capillary and it was exposed for 1 s at room temperature. No evidence of radiation damage was observed in any sample at this exposure. The 2D diffraction spectra were angularly integrated to get 1D intensity vs q patterns and the HEPES bulk solution was subtracted to the collected data. In order to calculate the electron density profiles, the integrated intensities of the diffraction peaks were determined by fitting the data with a series of Pearson IV functions using a nonlinear baseline.

3. Results and discussion

Hydration kinetics of DOPC multibilayers was followed in time due to the distinctive characteristics of EDXD [23]. At $t = 0$ an interlamellar separation $d = 52.9$ Å was calculated from the position of the Bragg peak maximum ($d = 2\pi/q$). The value of q was determined by fitting a Lorentz function to the peak. Reduced levels of hydration are responsible for oriented lipid membranes exhibiting smaller d-spacings with respect to the values reached under excess water conditions.

Upon progressive hydration, the water adsorption resulted in the continuous shift of the first-order Bragg maximum towards lower q-values as a consequence of the swelling of the DOPC membranes. Fig. 1 shows a comparison between the initial and final first-order Bragg peaks. During the sample hydration, the intensity of the first-order reflection decreases until the repeat spacing reaches its limiting value. At this point, further decrease of Bragg reflection intensity (data not reported) is indicative of water condensation on the sample. The interpretation of the observed effect is straightforward. The starting Bragg spacing corresponds to a number of ~14 water molecules per lipid molecule while the phosphocholine hydration shell is filled at ~12 waters per lipid [26]. Upon completion of the lipid hydration shell, structural changes in the lipid headgroup occurr while, at higher levels of hydration, the bilayer structure does not change any more as a function of hydration. Further adsorbed water molecules actually behave as bulk water promoting loss of spatial coherence and leading to a continuous lowering and broadening of the diffraction peaks.

The EDXD scan of DOPC multibilayers system in excess water condition is reported in Fig. 2a. The diffraction pattern shows strong first- and second-order Bragg peaks (0 0 l) of the liquid-crystalline lamellar structure of DOPC with a periodicity $d2\pi/q = 63.5$ Å. This finding confirms that aligned L_α DOPC multibilayers adsorbed to the silicon substrate effectively achieves a repeat

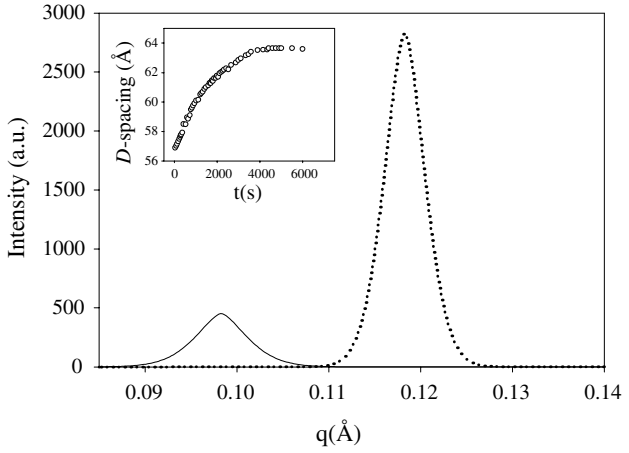

Fig. 1. Comparison between the initial (dotted line) and final (solid line) EDXD spectra in the hydration kinetics of solid-supported DOPC multibilayers system. Each pattern was collected for $t = 2$ s. In the inset the temporal evolution of the interlamellar d-spacing is reported.

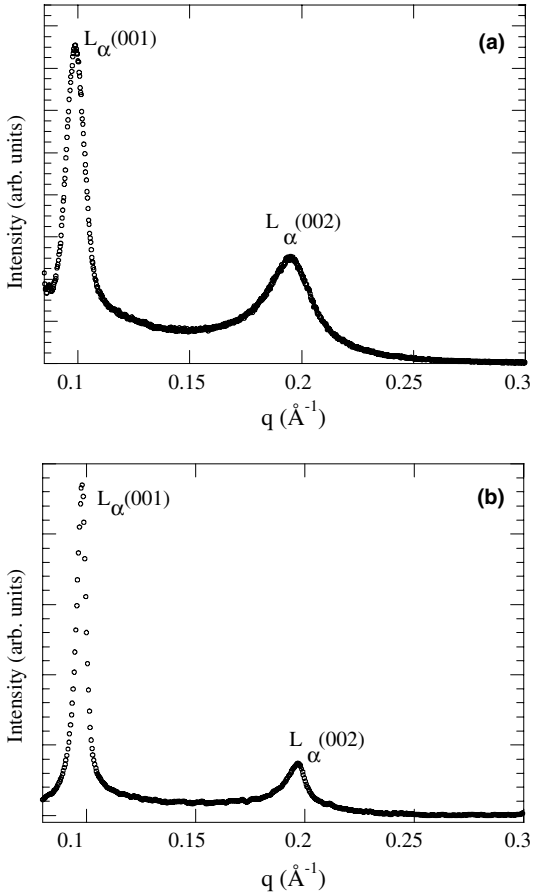

Fig. 2. EDXD pattern of fully hydrated DOPC multilamellar stack (panel a). The noticeable sharp reflections are the first- and second-order Bragg peaks (0 0 l), whereas the diffuse scattering is due to the random stacking disorder. Synchrotron XRD pattern collected on unoriented multilamellar DOPC liposomes is also reported (panel b).

d-spacing equivalent to ones found in liquid water. Indeed, two orders of diffraction are also observed for DOPC liposomes in bulk, as shown in Fig. 2b. This lamellar structure (L_α) has a spacing $d = 64.2$ Å, very close to the value of periodicity measured for the previous aligned DOPC multilayers sample. In both cases the presence of only two order of diffraction peaks reflects the strong fluctuation of the bilayers. The experimental findings for the adsorbed DOPC multilayers are somehow expected, since Katsaras unambigously showed that multibilayers systems, whether immersed in water or hydrated from vapor, can attain full hydration in all mesophases.

From the diffraction patterns of Fig. 2a, b we calculated the electron density profile along the normal to the bilayers of the DOPC. Due to the bilayer nature of the molecular arrangement, the electron density has a centre of symmetry in the middle of the bilayer. The electron density profile, $\Delta\rho$, along the normal to the bilayers, z, was then calculated as a Fourier sum of cosine terms,

$$\Delta\rho = \frac{\rho(z) - \langle\rho\rangle}{\left[\langle\rho^2(z)\rangle - \langle\rho\rangle^2\right]^{1/2}} = \sum_{l=1}^{N} F_l \cos\left(2\pi l \frac{z}{d}\right), \qquad (1)$$

where $\rho(z)$ is the electron density, $\langle\rho\rangle$ its average value, N is the highest order of observed reflections, F_l, is the form factor for the (0 0 l) reflection, d is the thickness of the repeating unit.

The discrete bilayer form factor is obtained from the integrated intensity $I_h = F_h^2/C_h$ under the hth diffraction peak, where C_h is the Lorentz-polarization correction factor. For a centrosymmetric and one-dimensional structure the form factor is a real number either positive or negative.

The phase problem, i.e. the choice of the best sign sequence for the structure factor, was solved using the approach originally proposed by Luzzati and co-workers [27,28]. The sign combination used to calculate the electron density profile is $- - + +$ relative to the structures factors F_1,F_2,F_3,F_4.

Fig. 3 shows the electron density profile over the unit cell of both solid-supported DOPC multilayers (continuous line) and unorientated DOPC liposomes (dotted line). The electron denser regions (i.e. the two maxima of Fig. 3) correspond to the phospholipid headgroups whereas the large central minimum corresponds to the region of the hydrocarbon tails. Therefore, the distance between the maxima of electron density provide a good estimate of the bilayer thickness d_{HH}. The lamellar d-spacing can be separated into the structural components, i.e. the bilayer thickness, d_{HH}, and water-layer thickness, d_W. Accordingly the interbilayer water thickness can be defined as $d_w = d - d_{HH}$.

From the continuous line of Fig. 3 we calculated the thickness of lipid bilayer, $d_{HH} = 35.6$ Å, and the water thickness $d_w = 27.9$ Å. The corresponding values for DOPC liposomes in bulk (dotted line) are $d_{HH} = 38.5$ and $d_w = 25.7$ Å. Comparison of the two profiles of Fig. 3 shows that the widths of electron density peaks associated to unoriented DOPC liposomes are wider compared to those of the oriented DOPC multilayers. This means that molecular disorder caused by bilayers fluctuations (either thermal or undulatory) is greater in the unoriented liposome than in fully hydrated solid-supported lipid multibilayers system [29]. This finding seems to be quite reasonable considering the mechanical constraints exerted by the solid support on the deposited multilayers. In spite of the limited resolution, the values obtained from the electron profiles are in good agreement with the structural data reported for fully hydrated DOPC bilayers [20,30].

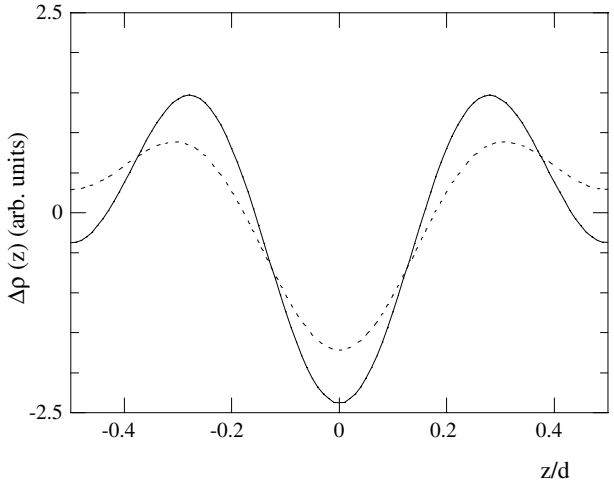

Fig. 3. Electron-density profile along the normal to the bilayers in the L_α phase corresponding to solid-supported DOPC multilayers (continuous line) and unorientated DOPC liposomes (dotted line).

Addition of DNA and Mn^{2+} to the DOPC solution produce major change in the structure of DOPC liposomes. Immediately after mixing, the solution was deposited onto the surface of a silicon wafer and allowed to dry. The dehydrated film was then hydrated from vapor exactly as for the DOPC multibilayers system. In Fig. 4a the series of four sharp Bragg reflections observed for the fully hydrated DOPC–DNA–Mn^{2+} triple complex is reported. A lamellar spacing $d_c = 73.6$ Å was calculated as $d_c = 2\pi n/q$, where n is the order of the Bragg peak and q is the transfer momentum determined by fitting a Lorentz function to each harmonic. Fig. 4b shows the synchrotron SAXS pattern of the unoriented liposome complex DOPC–DNA–Mn^{2+}, with the same molar ratio (3:4:12) used for the solid-supported samples. This pattern is characterized by two sets of peaks corresponding to distinct lamellar structures L_α and L_α^c, with spacing $d = 60.5$ and $d_c = 73$ Å, respectively. The former is the lamellar phase of pure DOPC and latter is the lamellar phase of the triple DOPC–DNA–Mn^{2+}

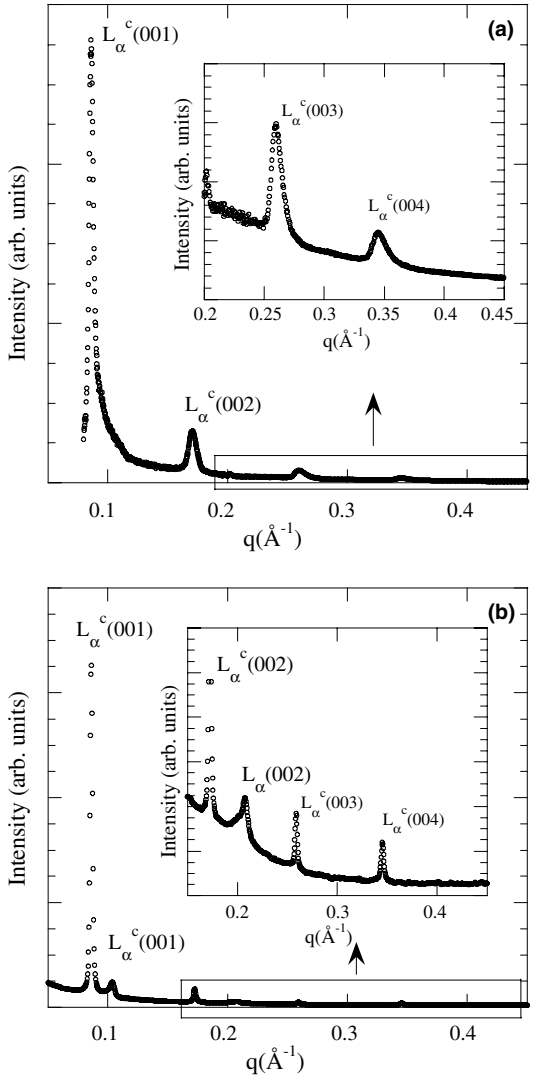

Fig. 4. EDXD (panel a) and synchrotron XRD (panel b) patterns of the L_α^c lamellar phase of (DOPC)–DNA–Mn^{2+} triple complexes. The synchrotron pattern shows coexistence of the L_α^c and L_α phase of pure DOPC.

complex. The appearance of diffraction peaks corresponding to uncomplexed lipid can be simply explained by considering the longer incubation time of the solid-supported sample. Indeed, this result confirms our previous findings (data not reported) that longer incubation times effectively result in higher percentage of complexed lipid. The structure of the complex is similar to that observed in cationic liposomes CL–DNA complexes, which are made of stacks of alternating lipid bilayers and DNA monolayers. It is important to observe that the value d_c corresponding to the lamellar spacing for the triple complexes in solution is in excellent agreement with the results obtained in the case of solid-supported complexes. It consists of flat lipid bilayers with DNA packed between them in a sandwich-like structures.

The L_α^c formation is promoted by the positively charged metal ions that bind the polar headgroups of DOPC with the negatively charged phosphate groups of DNA. The driving force for complex condensation is the release of counterions [4,5]. These complexes appear to be well ordered, with four plain Bragg peaks being detected. Diffraction peaks represent inter-bilayer coherence whereas the diffuse diffraction between them represents random stacking disorder. This multilayer-incoherent diffraction is lower in the case of the complex proving the high local order of the multilayered structure. In fact a decrease in the peak width is strongly indicative of increased order of the lipid molecules within the bilayers induced by DNA condensation. Fig. 5 shows the electron density profiles along the normal to the layers corresponding to the triple unoriented liposome complex (dotted line) and oriented solid-supported complex (continuous line). The structural parameters d_c, d-spacing of the unit cell, d_{HH} and d_w, bilayer and water thickness, are reported in Table 1.

The determined structural information are essentially the same both for solid-supported complexes and for the ones in solution. Analysis of Fig. 5 shows that the spreading of the density maxima due to the bilayer fluctuations is remarkably more pronounced in solution complexes. The same behaviour was observed for pure DOPC (Fig. 3). In liquid crystalline systems with very flexible lamellae, bilayer fluctuations may result from two distinct contributions, namely thermal fluctuations and whole-body undulatory motion of the individual layers related to the elastic properties [29,31]. As a thermal fluctuations are likely to play the same role in oriented solid-supported and unoriented solution samples, the sharpening of the density profile in Figs. 5 and 3 on going from unoriented to solid-supported sam-

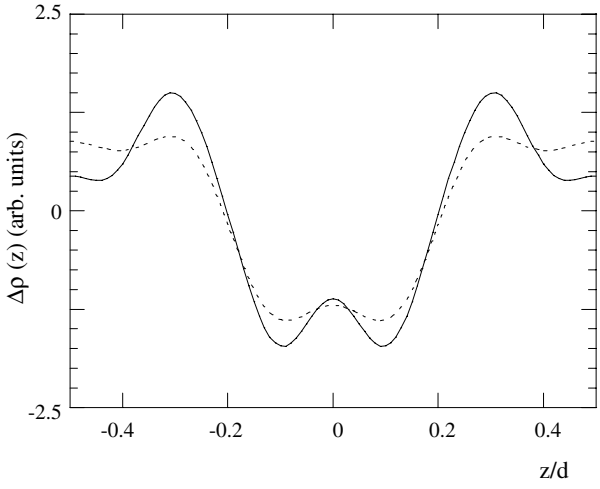

Fig. 5. Electron-density profile along the normal to the bilayers in the L_α^c phase of the triple complex DOPC:DNA:Mn^{2+} corresponding to solid-supported multilayers (continuous line) and unorientated liposomes (dotted line).

Table 1
Comparison between the structural parameters calculated for fully hydrated oriented complexes (A) and unoriented complexes in aqueous solution (B).

DOPC:DNA:Mn^{2+} 3:4:12	d_c (Å)	d_{HH} (Å)	d_w (Å)
A	73.6	44.9	28.7
B	73	44.1	28.9

ples can be interpreted as due to a change of the elastic properties (in particular an increase of the stiffness) driven by the solid support.

The complex investigated did not exhibit any DNA diffraction peak associated with DNA–DNA spatial in plane correlation. In the case of the XRD measurements in solution the absence of this peak can be justified considering the higher mobility of the fusogenic agent, i.e. metal ions, that does not induce enough constraint to allow the DNA strands assume a regular packing within the lipid bilayer.

4. Conclusions

In conclusion, the proposed experimental procedure resulted in the formation of solid-supported DOPC–DNA–Mn^{2+} triple complexes in the relevant excess water condition. The inner structure of solid-supported complexes was characterized by EDXD and found to be essentially the same as their counterpart in aqueous solution. As a result, solid-supported complexes can emerge as an interesting measurement condition in order to retrieve high-resolution structural information on triple L–DNA–Me^{2+} complexes.

References

[1] P.L. Felgner, T.R. Gadek, M. Holm, R. Roman, H.W. Chan, M. Wenz, J.P. Northrop, G.M. Ringold, M. Danielsen, Proc. Natl. Acad. USA 84 (1987) 7413.
[2] P.L. Felgner, Sci. Am. 276 (1997) 102.
[3] D.D. Lasic, CRC Press, Boka Raton, FL, 1997.
[4] R. Podgornik, Nancy Smith Templeton (Eds.), Gene and Cell Therapy, 2004.
[5] K. Wagner, D. Harries, S. May, V. Kahl, J.O. Rädler, A. Ben Shaul, Langmuir 16 (2000) 303.
[6] T. Salditt, I. Koltover, J.O. Rädler, C.R. Safinya, Science 275 (1997) 810.
[7] T. Salditt, I. Koltover, J.O. Rädler, C.R. Safinya, Phys. Rev. Lett. 79 (1997) 2582.
[8] T. Salditt, I. Koltover, J.O. Rädler, C.R. Safinya, Phys. Rev. E 58 (1998) 889.
[9] I. Koltover, T. Salditt, C.R. Safinya, Biophys. J. 77 (1999) 915.
[10] G. Caracciolo, R. Caminiti, F. Natali, A. Congiu Castellano, Chem. Phys. Lett. 366 (2002) 200.
[11] G. Caracciolo, D. Pozzi, R. Caminiti, A. Congiu Castellano, Eur. Phys. J. E 10 (2003) 331.
[12] F. Sakurai, R. Inoue, Y. Nishino, A. Okuda, O. Matsumoto, T. Taga, F. Yamashita, Y. Takakura, M. Hashida, J. Control. Release 66 (2000) 255.
[13] S.W. Hui, M. Langner, Y.L. Zhao, P. Ross, E. Hurley, K. Chan, Biophys. J. 71 (1996) 590.
[14] K.W. Mok, P.R. Cullis, Biophys. J. 73 (1998) 2534.
[15] I. Koltover, T. Salditt, J.O. Rädler, C.R. Safinya, Science 281 (1998) 78.
[16] J.J. McManus, J.O. Rädler, K.A. Dawson, J. Phys. Chem. B 107 (36) (2003) 9869.
[17] J.J. McManus, J.O. Rädler, K.A. Dawson, Langmuir 19 (23) (2003) 9630.
[18] V.G. Budker, A.A. Godovikov, L.P. Naumova, I.A. Slepneva, Nucleic Acids Res. 8 (11) (1980) 2499.
[19] J. Marra, J. Israelachvili, Biochemistry 24 (1985) 4608.
[20] O. Francescangeli, V. Stanic, L. Gobbi, P. Bruni, M. Iacussi, G. Tosi, S. Bernstorff, Phys. Rev. E 67 (2003) 011904.
[21] J. Katsaras, Biophys. J. 75 (1998) 2157.
[22] J. Katsaras, M.J. Watson, Rev. Sci. Instrum. 71 (4) (2000) 173.
[23] R. Caminiti, V. Rossi Albertini, Int. Rev. Phys. Chem. 8 (2) (1999) 263.
[24] G. Caracciolo, R. Caminiti, D. Pozzi, M. Friello, F. Boffi, A. Congiu Castellano, Chem. Phys. Lett. 351 (2002) 222.
[25] G. Caracciolo, G. Amiconi, L. Bencivenni, G. Boumis, R. Caminiti, E. Finocchiaro, B. Maras, Paolinelli, A. Congiu Castellano, Eur. Biophys. J. 30 (2001) 163.
[26] K. Hristova, S. White, Biophys. J. 74 (1998) 2419.
[27] V. Luzzati, P. Mariani, H. Delacroix, Makromol. Chem., Macromol. Symp. 15 (1998) 1.
[28] O. Francescangeli, D. Rinaldi, M. Laus, G. Galli, B. Gallot, J. Phys. II France 6 (1996) 77.
[29] O. Francescangeli, V. Stanic, D.E. Lucchetta, P. Bruni, M. Iacussi, F. Cingolani, Mol. Cryst. Liq. Cryst. 398 (2003) 259.
[30] S. Tristram-Nagle, H. Petrache, J.F. Nagle, Biophys. J. 75 (1998) 917.
[31] C.R. Safinya, in: T. Riste, D. Sherington (Eds.), Phase Transition in Soft Condensed Matter, Plenum Publishing, New York, 2000, p. 249.